Available online at www.sciencedirect.com

ScienceDirect

ELSEVIER

Nuclear and Particle Physics Proceedings 00 (2016) 1–6

Nuclear and Particle Physics Proceedings

ATL-PHYS-PROC-2016-158
02 October 2016

Measurements of $t\bar{t}$+X using the ATLAS detector

Bárbara Álvarez González (CERN)

On behalf of the ATLAS Collaboration

Abstract

The large centre-of-mass energy available at the LHC proton-proton collider allows for copious production of top-quark pairs in association with other final state particles at high transverse momentum. Results on the top-quark pair production in association with W and Z bosons at both 8 and 13 TeV are presented as well as the measurement of the cross section for production with an associated isolated photon at 7 TeV. The ATLAS experiment has measured several final state observables that are sensitive to additional radiation in top anti-top quark final states. Analyses probing the top-quark pair production with additional QCD radiation include the multiplicity of jets for various transverse momentum thresholds in the 13 TeV data. These measurements are compared to some of the most recent Monte Carlo event generators based on NLO QCD or LO multi-leg matrix element calculations.

Keywords: ATLAS, top, cross section, precision measurement

1. Introduction

This paper presents a collection of recent results ranging from the $t\bar{t}V$ ($V = W$ or Z) production at $\sqrt{s} = 13$ and 8 TeV, to measurements of jets produced in association with $t\bar{t}$ pairs at $\sqrt{s} = 13$ and 8 TeV, and of b-jets as well as the measurement of the $t\bar{t}$ production cross section associated with an isolated photon at 7 TeV.

2. Measurements in pp collisions at $\sqrt{s} = 13$ TeV

The results presented in this section use a data sample corresponding to a total integrated luminosity of 3.2 fb^{-1} collected by the ATLAS experiment [1] in 2015 at the LHC.

2.1. Measurement of $t\bar{t}$+W/Z production cross sections

The production rate of a top-quark pair with a massive vector boson could be altered in the presence of physics beyond the Standard Model (SM)[2, 3], and therefore the measurements of the associated production of $t\bar{t}$ with a Z boson ($t\bar{t}Z$) and a W boson ($t\bar{t}W$) are important checks for the validity of the SM.

A preliminary measurement of the $t\bar{t}Z$ and $t\bar{t}W$ production cross sections in final states with either two same-charge muons, or three or four leptons (electrons or muons) [4] is presented. Examples of Feynman diagrams for these processes are shown in Fig. 1. Each

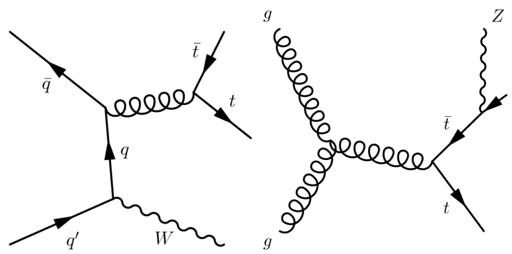

Figure 1: Examples of Feynman diagrams for the production of $t\bar{t}$ in association with W and Z bosons [5].

channel is divided in multiple analysis regions depending on the number of jets, b-jets and Z-boson mass windows in order to enhance the sensitivity to the signal.

In order to extract the $t\bar{t}Z$ ($t\bar{t}W$) cross section, eight (two) signal regions and two (two) background control regions are fitted simultaneously. The production cross sections are determined using binned maximum-likelihood fits to the numbers of events in the signal regions, assuming the SM cross section and its predicted uncertainty at next-to-leading order (NLO) in QCD for the other signal process. The fits are based on the profile likelihood technique, where systematic uncertainties are allowed to vary in the fits as nuisance parameters. None of the uncertainties are found to be significantly constrained or pulled from their initial values.

The measured cross sections are: $\sigma_{t\bar{t}Z} = 0.9 \pm 0.3$ pb and $\sigma_{t\bar{t}W} = 1.4 \pm 0.8$ pb in agreement with the SM predictions at NLO QCD, $t\bar{t} + Z = 0.76 \pm 0.08$ pb and $t\bar{t} + W = 0.57 \pm 0.06$ pb, computed using MadGraph5_aMC@NLO [6]. Both results are dominated by statistical uncertainties. Fig. 2 and 3 show the expected yields after the fits compared to data for the $t\bar{t}Z$ and $t\bar{t}W$ fit, respectively, in the relevant signal regions and the two control regions used to constrain the WZ and ZZ backgrounds.

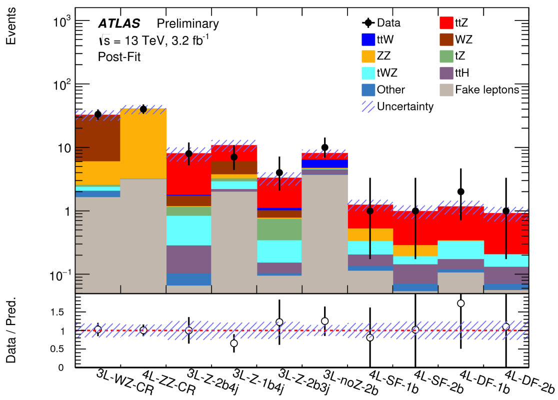

Figure 2: Expected yields after the fit compared to data for the $t\bar{t}$+Z fit. The lower part of the figure shows the ratio of data to prediction. The hatched area corresponds to the total uncertainty on the predicted yields [4].

2.2. Measurement of jets produced in top quark events

This section presents the measurement of jets associated to $t\bar{t}$ events, using the dilepton final state with two b-tagged jets [7]. These measurements represent the normalized differential cross sections of top-quark pair production as a function of the multiplicity of additional jets unfolded at particle level.

The production of additional jets in $t\bar{t}$ events arises from higher-order perturbative QCD effects. The uncertainties associated with these processes are significant both for precision measurements and for many searches for new physics phenomena where $t\bar{t}$ production with additional jets is a dominant background. The aim of this analysis is to test several theoretical approaches that model the production of $t\bar{t}$ events with additional jets, including NLO QCD calculations, parton-shower models and methods matching fixed-order QCD calculations with the parton shower.

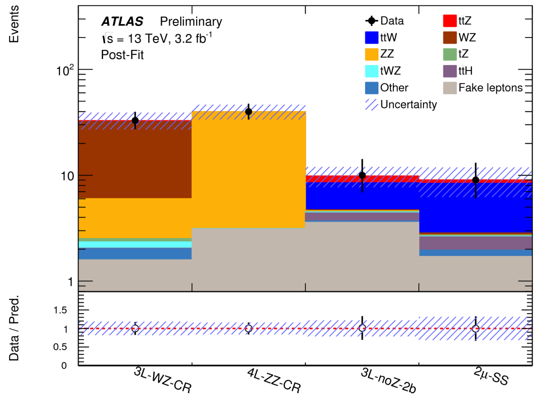

Figure 3: Expected yields after the fit compared to data for the $t\bar{t}$+W fit. The lower part of the figure shows the ratio of data to prediction. The hatched area corresponds to the total uncertainty on the predicted yields [4].

The jet multiplicity for the additional jets is obtained for various jet transverse momentum thresholds: 25, 40, 60 and 80 GeV, and Fig. 4 shows the reconstructed multiplicity distribution for the 25 GeV threshold.

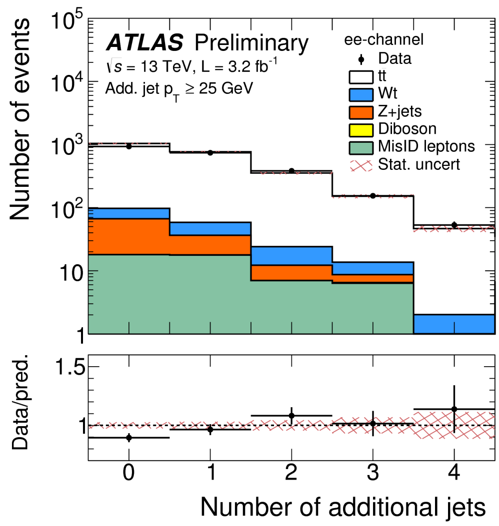

Figure 4: Distributions of the reconstructed multiplicity of jets associated to $t\bar{t}$ pairs with p_T >25 GeV. Data are compared to the baseline $t\bar{t}$ and background simulations. The lower part of the figure shows the ratio of data to prediction. Uncertainties are statistical only [7].

The unfolded results are compared to predictions of different NLO Monte Carlo models as shown in Fig. 5 and to variations of initial- and final-state radiation within Powheg+Pythia6. In general, there is agreement between the data and the predictions within the current experimental uncertainties. However, the Powheg+Pythia6 predictions are systematically below the data at high multiplicity. In addition, among the different shower variations the settings leading to more radiation describe the data best, as described in Ref. [7].

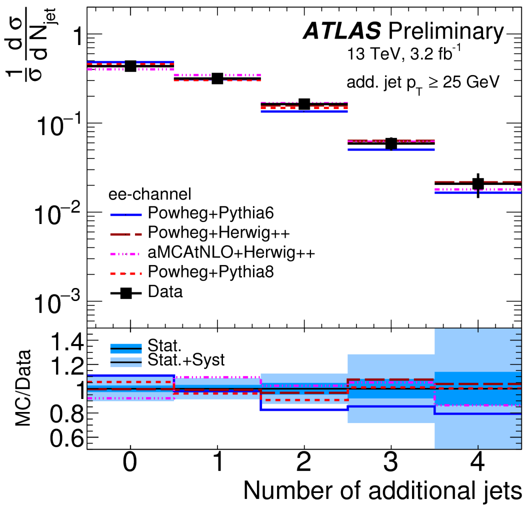

Figure 5: Unfolded jet multiplicity distribution for additional jets with $p_T > 25$ GeV and different $t\bar{t}$ decay channels with statistical uncertainty (dark blue band) and total uncertainty (light blue band). Data are compared to predictions of different shower generators interfaced with Powheg and aMC@NLO as an alternative NLO MC model. The lower part of the figure shows the ratio of simulation to data [7].

3. Measurements in pp collisions at $\sqrt{s}$ = 8 TeV

The analyses described in this section are performed using a dataset with an integrated luminosity of 20.3 fb^{-1} collected by the ATLAS experiment in 2012 at $\sqrt{s}$ =8 TeV.

3.1. Measurement of $t\bar{t}$+W/Z production cross sections

A measurement of the $t\bar{t}Z$ and $t\bar{t}W$ production cross sections in final states with either two same-sign (2LSS) and opposite-sign (2LOS) leptons, three (3L) or four leptons (4L) [5] is presented. Control regions are also defined to constrain the main backgrounds: $t\bar{t}$ for 2LOS, Z+jets for 2LOS, WZ for 3L and ZZ for the 4L signal region.

The $\sigma_{t\bar{t}+W}$ and $\sigma_{t\bar{t}+Z}$ are simultaneously extracted using a maximum likelihood fit over five control regions and fifteen signal regions: three signal regions in the opposite-sign dilepton channel, three signal regions in the same-sign dilepton channel, four signal regions in the three-lepton channel and five signal regions in the four-lepton channel. Fig. 6 shows the expected yields after the fit compared to data in the signal and the control regions.

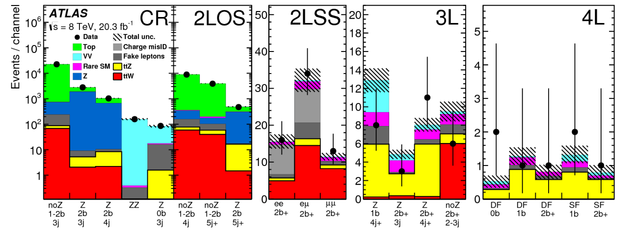

Figure 6: Expected yields after the fit compared to data in the five control regions (CR) and the fifteen signal regions [5].

The measured cross sections are:

$$\sigma_{t\bar{t}+W} = 369\,^{+86}_{-79}\,(\text{stat}) \pm 44\,(\text{syst})\,\text{fb} = 369\,^{+100}_{-91}\,\text{fb and}$$
$$\sigma_{t\bar{t}+Z} = 176\,^{+52}_{-48}\,(\text{stat}) \pm 24\,(\text{syst})\,\text{fb} = 176\,^{+58}_{-52}\,\text{fb.}$$

All measurements are consistent with the NLO QCD theoretical calculations for $t\bar{t}W$ and $t\bar{t}Z$ processes, $\sigma_{t\bar{t}+W} = 232 \pm 32$ fb and $\sigma_{t\bar{t}+Z} = 215 \pm 30$ fb [6], as shown in Fig. 7.

The $t\bar{t}Z$ and $t\bar{t}W$ processes have been observed by ATLAS using the Run-1 dataset at 8 TeV, with measured cross sections compatible with the SM predictions and uncertainties of 30%.

3.2. Fiducial cross sections for $t\bar{t}$ with additional b-jets

The measurement of $t\bar{t}$ in association with one or more b-jets is important in providing a more detailed understanding of QCD, initial state radiation. This process represents the largest background to the search for $t\bar{t}H$ production in $H \to b\bar{b}$.

The fiducial cross sections for $t\bar{t}$ with one or two additional b-jets are presented in Ref. [8]. For the $t\bar{t}$+b, the lepton plus jets and dilepton ($e\mu$) channels are used and the analysis strategy follows a fit to a multivariate b-tagging discriminant defined to identify b-jets

For $t\bar{t}$+$b\bar{b}$, only the dilepton channel is used (ee, $\mu\mu$, $e\mu$) and two strategies are followed: a cut-based analysis requiring four b-jets and a fit to a multivariate b-tagging discriminant with looser requirements. The b-tagging discriminant distribution is shown in Fig. 8 after the fit is performed.

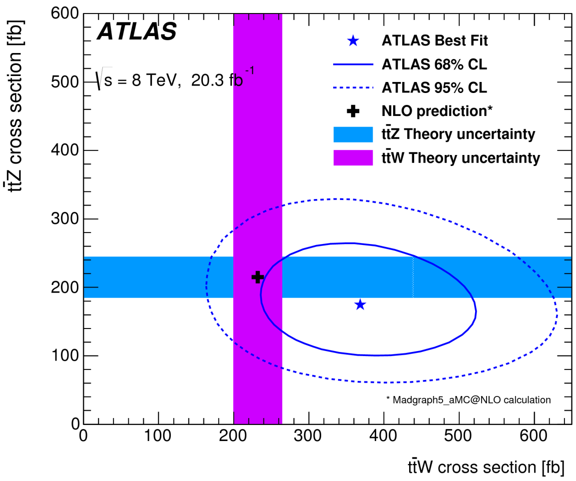

Figure 7: The result of a simultaneous fit to the $t\bar{t}W$ and $t\bar{t}Z$ cross sections along with the 68% and 95% CL uncertainty contours. Also shown are the theory predictions at NLO in QCD where the shaded bands represent the theoretical uncertainties, which cover the renormalization and factorization scale uncertainties as well as PDF uncertainties including α_s variations [5].

The measured fiducial cross sections for $t\bar{t}$+b in the lepton-plus-jets and dilepton channels, and for $t\bar{t}$+$b\bar{b}$ in the dilepton channel using the cut-based or the fit-based method are shown in Table 1 together with the predicted cross-sections from PowhegBox+Pythia6 [9] for the QCD component, from Helac [10] for $t\bar{t}H$ and from MadGraph5 [11] for $t\bar{t}V$. The result for the ratio measurement of $t\bar{t}$ production with two additional b-jets to $t\bar{t}$ production with any two additional jets, R_{ttbb}, using the fit-based method is also shown. The uncertainties quoted are from the statistical and total systematic uncertainties. The measurements are presented after

Table 1: Measured fiducial cross section for $t\bar{t}$+b in the lepton-plus-jets and dilepton channels, and $t\bar{t}$+$b\bar{b}$ in the dilepton channel. The result for the ratio measurement R_{ttbb} is also shown [8].

Analysis	Measured Cross-section [fb]	Predicted Cross-section [fb]
$\sigma_{ttb\,\mathrm{lepton-plus-jets}}$	950 ± 70 (stat.) $^{+240}_{-190}$ (syst.)	720
$\sigma_{ttb\,e\mu}$	50 ± 10 (stat.) $^{+15}_{-10}$ (syst.)	38
$\sigma_{ttbb\,\mathrm{cut-based}}$	19.3 ± 3.5 (stat.) ± 5.7 (syst.)	12.3
$\sigma_{ttbb\,\mathrm{fit-based}}$	13.5 ± 3.3 (stat.) ± 3.6 (syst.)	12.3
R_{ttbb}	1.30 ± 0.33 (stat.) ± 0.28 (syst.) %	1.27 %

subtracting the EWK contribution, to compare to NLO pQCD theory predictions. The main uncertainties are due to the impact of the b-tagging scale factor uncertainties and the choice of MC generator which is derived by comparing $t\bar{t}$ samples generated with Madgraph interfaced with Pythia6 to the baseline sample generated with Powheg+Pythia6. These results are also shown in Fig. 9 compared to theoretical predictions obtained with several generators.

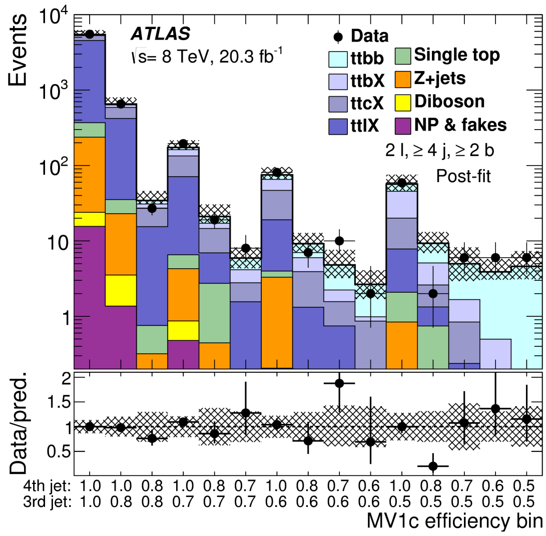

Figure 8: The MV1c distribution of jets with the third and fourth highest MV1c weight in the dilepton channel for all signal and background components. The lower part of the figure shows the ratio of data to prediction [8].

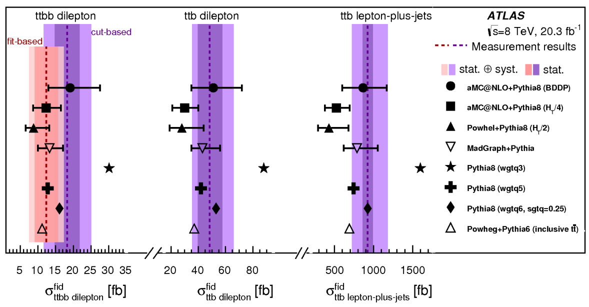

Figure 9: Comparison of the measured cross sections in the three fiducial phase-space regions with theoretical predictions obtained from a variety of different generators [8].

3.3. Measurement of jets produced in top-quark events

The measurements of the jet activity in $t\bar{t}$ events are presented in Ref. [12]. The events were selected in the dilepton ($e\mu$) channel with two b-jets.

The normalized differential cross sections for top-quark pair production as a function of the multiplicity of additional jets unfolded at particle level are obtained as described in Sec. 2.2. The gap fraction, the fraction of events which do not contain an additional jet in the central rapidity region ($|y| < 2.1$), was also measured for several rapidity and $m_{e\mu b\bar{b}}$ intervals.

The measured gap fraction as a function of Q_0 in the veto-region rapidity interval $|y| < 0.8$ is shown in Fig. 10. The data are shown as the points with error bars indicating the total uncertainty, and compared to the predictions from various $t\bar{t}$ simulation samples shown as smooth curves. The lower plots show the ratio of predictions to data, with the data uncertainty being indicated by the shaded band, and the Q_0 thresholds corresponding to the left edges of the histogram bins, except for the first bin. All measurements are in good agreement with NLO and LO predictions. These results can be used to optimize the choice of QCD scale and parton shower parameters in $t\bar{t}$ generators.

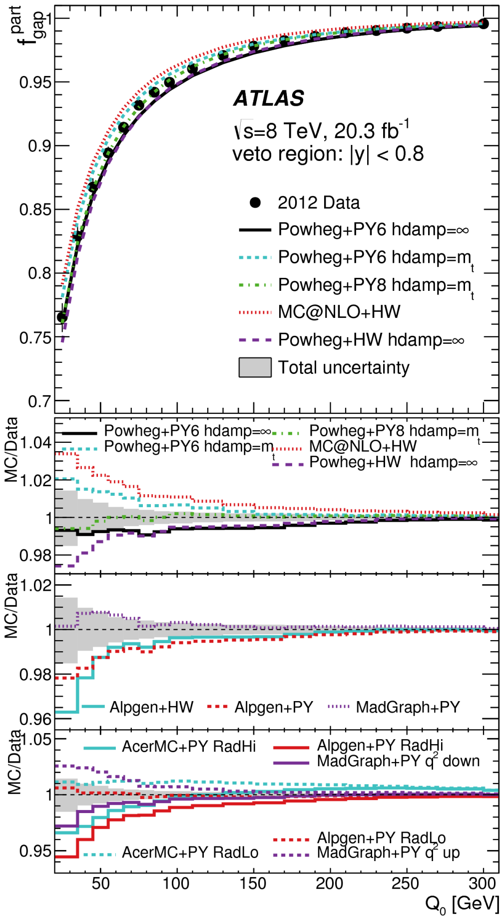

Figure 10: The measured gap fraction $f(Q_0)$ in $t\bar{t}$ events, as a function of Q_0 in the veto-region rapidity interval $|y| < 0.8$. The lower part of the figure shows the ratios of simulation to data [12].

4. Measurements in pp collisions at $\sqrt{s}$ = 7 TeV

4.1. Observation of $t\bar{t}$ in association with a photon

The measurement of top-quark pair production in association with a photon can constrain models of new physics, for example those with composite top quarks [13] or with excited top-quark production. The observation of $t\bar{t}\gamma$ in proton-proton collisions at a centre-of-mass energy of $\sqrt{s}$= 7 TeV with 4.59 fb^{-1} is presented in Ref. [14]. The analysis is performed on $t\bar{t}$ candidate events in the lepton plus jets final state with one additional photon of $E_T > 20$ GeV. The cross-section measurement is made within a fiducial kinematic region corresponding to the ATLAS acceptance, as described in Ref. [14].

The measurement of the $t\bar{t} + \gamma$ production cross section is done using a template profile likelihood fit, where the photon track-isolation is the discriminating variable. This variable, shown in Fig. 11, is defined as the scalar sum of the transverse momenta of selected tracks in a cone of $\Delta R = 0.2$ around the photon candidate. The measured $t\bar{t}\gamma$ fiducial cross section is:

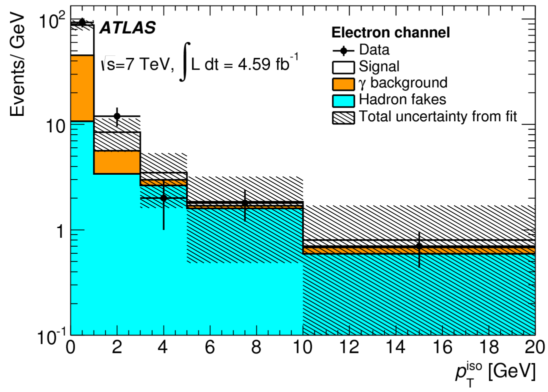

Figure 11: Results of the combined likelihood fit using the track-isolation (p_T^{iso}) distributions as the discriminating variable. The contribution from $t\bar{t}$ events is labeled as 'Signal', prompt-photon background is labeled 'γ backgrounds', the contribution from hadrons misidentified as photons (as estimated by the template fit) is labeled as 'Hadron fakes' [14].

$$\sigma^{fid}_{t\bar{t}+\gamma}\ x\ BR(t\bar{t} \to lj) = 63 \pm 8\ \text{(stat)}\ ^{+17}_{-13}\ \text{(syst)} \pm 1\ \text{(lumi) fb.}$$

The dominant source of systematic uncertainties is due to jet modeling, the largest uncertainty arising from the jet energy scale of about 15%. The result is in good agreement with the NLO predicted cross section. The process is observed with a significance of 5.3σ.

5. Summary

Various measurements related to top-quark pair production have been carried out with the ATLAS experiment at the LHC at different centre-of-mass energies. All measurements are consistent with the SM predictions at NLO in QCD and the preliminary Run-2 measurements are currently statistically limited. These results are used to optimise the $t\bar{t}$ MC generator predictions and their parameters.

References

[1] ATLAS Collaboration, JINST, 3 (2008) S08003
[2] R. Chivukula, E. H. Simmons and J. Terning, Phys. Lett. B 331 (1994) 383
[3] M. Perelstein, Prog. Part. Nucl. Phys. 58 (2007) 247
[4] ATLAS Collaboration, ATLAS-CONF-2016-003, https://cds.cern.ch/record/2138947
[5] ATLAS Collaboration, JHEP11 (2015) 172
[6] J. Alwall et al., JHEP 07 (2014) 079, arXiv: 1405.0301
[7] ATLAS Collaboration, ATLAS-CONF-2015-065, https://cds.cern.ch/record/2114832
[8] ATLAS Collaboration, Eur. Phys. J. C (2016) 76:11
[9] P. Nason, JHEP11 (2004) 040, arXiv:hep-ph/0409146
[10] G. Bevilacqua et al., Comput. Phys. Commun. 184 (2013) 986, arXiv:1110.1499v2 [hep-ph]
[11] J. Alwall et al., JHEP 09 (2007) 028, arXiv:0706.2334 [hep-ph]
[12] ATLAS Collaboration, arXiv:1606.09490
[13] B. Lillie, J.Shu, and T.M.P. Tait, JHEP04 (2008) 087
[14] ATLAS Collaboration, PRD 91 (2015) 072007